Check for updates

ACES Asian Chemical Editorial Society

doi.org/10.1002/cnma.202100359

CHEMNANOMAT
Full Paper

An Efficient Method for Covalent Surface Functionalization of Ultrasmall Metallic Nanoparticles by Surface Azidation Followed by Copper-Catalyzed Azide-Alkyne Cycloaddition (Click Chemistry)

Kai Klein,[a] Kateryna Loza,[a] Marc Heggen,[b] and Matthias Epple*[a]

Abstract: The azidation of glutathione (GSH)-functionalized ultrasmall gold nanoparticles (2 nm) by the azide transfer reagent imidazole-1-sulfonyl azide hydrogen sulfate leads to azide-terminated nanoparticles with high yield. A subsequent copper-catalyzed azide-alkyne cycloaddition (CuAAC), i.e. a click reaction, leads to covalently functionalized nanoparticles. This was demonstrated with two alkyne-functionalized dyes, i.e. FAM-alkyne and AlexaFluor-647-alkyne, that were covalently coupled to the nanoparticles. The integrity of the glutathione ligand and the successful surface azidation were demonstrated by one-dimensional and two-dimensional NMR spectroscopy. The surface composition of the nanoparticles was determined by quantitative NMR spectroscopy and UV/vis spectroscopy. Each nanoparticle carries 125 glutathione molecules of which 118 were substituted by an azide group. After dye conjugation, either 6 FAM molecules or 11 AlexaFluor-647 molecules were present on each nanoparticle, respectively. The dye-clicked nanoparticles were highly fluorescent due to the absence of surface plasmon resonance. The post-functionalization of GSH avoids a chemical reaction of a functional ligand during the reduction reaction, gives a high yield (up to 50 mg nanoparticles per batch), is based on water as solvent, and is applicable for metallic nanoparticles in general.

Introduction

Ultrasmall gold nanoparticles have gained a considerable degree of attention because of their small size which inter alia permits an easy penetration through cell membranes and sometimes even nuclear membranes.[1] Depending on the ligand, they possess an inherent autofluorescence that can be used for intracellular detection.[2] If they are used for a theranostic purpose, e.g. for imaging, drug delivery, or protein targeting, it is a prerequisite that all attached ligands, functional or stabilizing, remain firmly attached to the nanoparticle surface. This must be the case both during synthesis and during application e.g. after cellular uptake. This calls for a covalent bond between metal and ligand instead of a purely adsorptive coating. The strong gold-sulfur bond is very stable under most circumstances,[3] and the somewhat weaker gold-phosphorous bond[4] has also been applied in many cases. Usually, the Brust-Schiffrin synthesis that involves the reduction of $HAuCl_4$ with $NaBH_4$ is used to prepare ultrasmall gold nanoparticles.[5]

A controlled surface functionalization of gold nanoparticles is possible in three different ways.[6] In the first approach, a thiol-containing ligand is attached during the reduction of gold ions to elemental gold. While this works for chemically robust ligands like some peptides or polymers,[7] the harsh reaction conditions (presence of oxidizing Au^{+III} and of reducing $NaBH_4$) can induce unwanted side reactions in the ligand. For instance, a reagent for an azide surface functionalization is the azide-terminated tripeptide K(N_3)CD,[8] However, it was shown that about 50% of the azide groups were reduced to amine groups during the gold reduction, thereby rendering the system less well defined.[8b] The second approach involves the subsequent exchange of a ligand that was used during the reduction reaction (e.g. cysteine, glutathione, tiopronine) by another thiol-containing ligand.[9] Although this is generally possible, questions remain about the rate and the quantitative nature (100% is a prerequisite for a well-defined system) of the ligand exchange. The third approach involves a covalent surface functionalization of a previously attached ligand.[8,10] For this, a suitable functional group must be present on the nanoparticle for subsequent functionalization.

The well-established copper-catalyzed azide-alkyne cycloaddition (CuAAc)[11] is a prominent example for a click reaction[12] that can be used to functionalize nanoparticles, including gold nanoparticles.[6,10a,13] Here we demonstrate how the amine groups of glutathione-functionalized ultrasmall gold nanoparticles can be almost quantitatively converted to azide groups that can then be used for a subsequent CuAAC click reaction. This was demonstrated with two alkyne-terminated dyes, followed by an in-depth characterization of the nanoparticles by NMR spectroscopy and transmission electron micro-

[a] K. Klein, Dr. K. Loza, Prof. Dr. M. Epple
Inorganic Chemistry and Centre for Nanointegration Duisburg-Essen (CeNIDE)
University of Duisburg-Essen
Universitaetsstr. 5–7, 45117 Essen (Germany)
E-mail: matthias.epple@uni-due.de

[b] Dr. M. Heggen
Ernst Ruska Centre for Microscopy and Spectroscopy with Electrons
Forschungszentrum Jülich GmbH
52428 Jülich (Germany)

Supporting information for this article is available on the WWW under https://doi.org/10.1002/cnma.202100359

© 2021 The Authors. ChemNanoMat published by Wiley-VCH GmbH. This is an open access article under the terms of the Creative Commons Attribution Non-Commercial NoDerivs License, which permits use and distribution in any medium, provided the original work is properly cited, the use is non-commercial and no modifications or adaptations are made.

scopy, including the quantification of the number of clicked molecules. The reaction yield is at least 50 mg per batch, making this a broadly applicable method for a covalent surface functionalization of water-dispersible gold nanoparticles.

Results and Discussion

First, glutathione-functionalized ultrasmall gold nanoparticles (denoted as AuGSH in the following) were prepared according to the standard Brust-Schiffrin synthesis.[5b] In the next step, the amine group in AuGSH nanoparticles was substituted by an azide group with an azide-transfer reagent,[14] leading to AuGSH-N_3 nanoparticles. Figure 1 shows the main reaction steps.

AuGSH and AuGSH-N_3 nanoparticles were thoroughly characterized by UV/vis spectroscopy, IR spectroscopy, high-resolution transmission electron microscopy (HRTEM), differential centrifugal sedimentation (DCS), and NMR spectroscopy. The UV spectra did not show a surface plasmon resonance (SPR) band,[15] i.e. the sample did not contain larger (plasmonic) gold nanoparticles (Figure 2). Ultrasmall nanoparticles of 2 nm are too small for a surface plasmon resonance.[1]

Infrared spectroscopy (IR) on lyophilized nanoparticles showed the successful substitution of amine by azide on the nanoparticle surface (evolution of the N_3 stretching vibration at 2106 cm^{-1}; Figure 3).

Differential centrifugal sedimentation (DCS) confirmed the good dispersibility of the nanoparticles and the absence of agglomeration with a hydrodynamic diameter below 2 nm (Figure 4). Note that DCS systematically underestimates the hydrodynamic particle diameter due to the ligand shell.[16] The size of the nanoparticles did not change after azidation according to UV-vis and DCS results. In particular, no agglomeration had occurred as evident by the DCS results and the absence of a scattering signal in dynamic light scattering (DLS; data not shown).

High-resolution transmission electron microscopy (HR-TEM) showed the diameter of the metallic core and confirmed the absence of larger nanoparticles (Figure 5). It also showed the internal crystallinity and a reasonably good monodispersity, in agreement with the DCS results. As expected, the gold core was not affected by the covalent surface functionalization.

The nature of the surface of ultrasmall nanoparticles can be conveniently probed by NMR spectroscopy.[17] This is a major advantage because it allows to identify and to quantify the attached ligands, in our case before and after surface azidation. However, the peaks of the ligands on the nanoparticle surface are generally broadened due to the vicinity of the metallic core. The still comparatively narrow NMR signals demonstrate that the nanoparticles did not significantly agglomerate after the surface functionalization. To fully characterize the particles and to quantify the efficiency of the surface reaction, we have carried out an extensive NMR characterization. Figure 6 shows the ^{1}H-NMR spectra of AuGSH and AuGSH-N_3 nanoparticles that are very similar and indicate that the GSH molecules on the surface were still intact. The signals of the glutamic acid protons H4 and H5 were clearly visible at 2.55 and 2.20 ppm. The H2 protons were within the water suppression around 4.6 ppm. The signal for H3 was strongly broadened as this is closest to the metal core. The peaks of H1 and H6 were merged into one broad signal at around 3.8 ppm.

Further NMR characterization data, including 2D NMR spectra, clearly confirmed that the reaction had occurred as

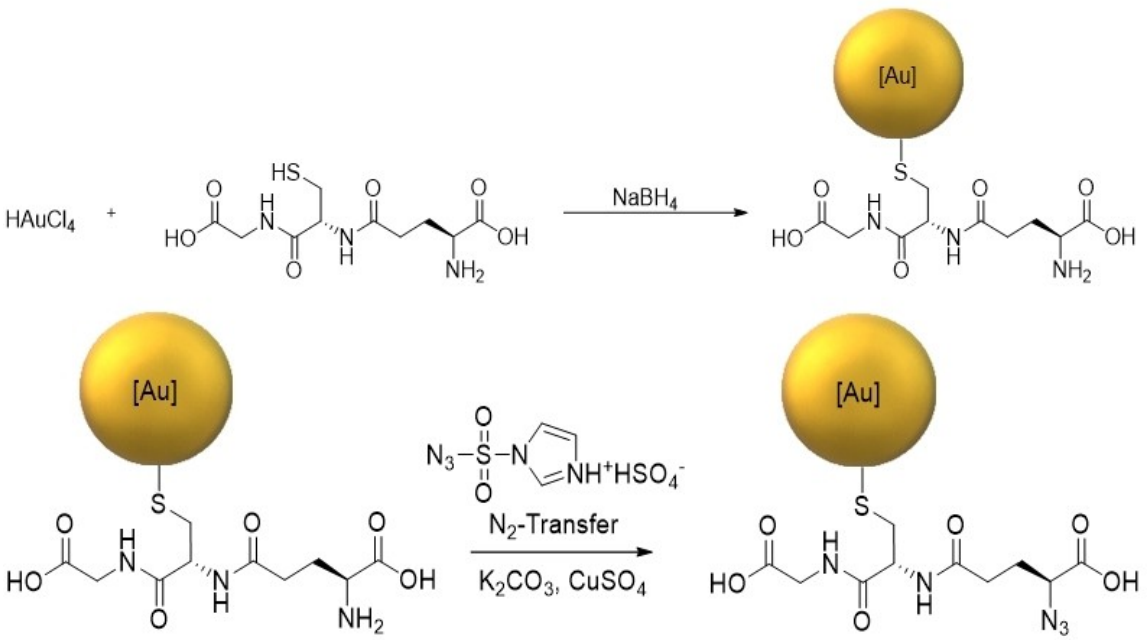

Figure 1. Synthetic pathways to AuGSH (**top**) and AuGSH-N_3 nanoparticles (**bottom**). The amine group of GSH is converted into an azide group by a copper-catalyzed N_2 transfer reaction.

© 2021 The Authors. ChemNanoMat published by Wiley-VCH GmbH

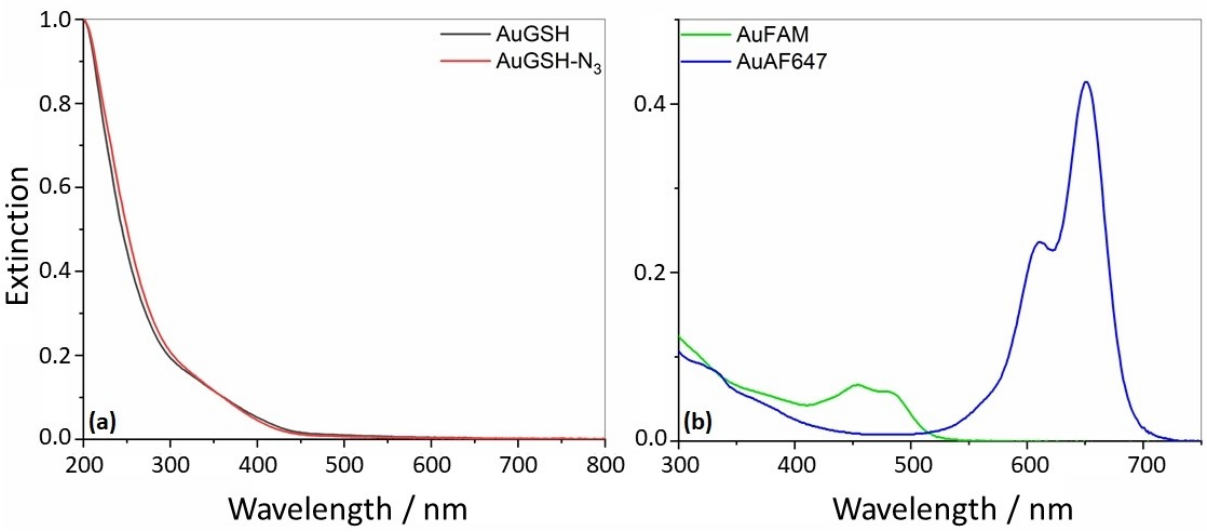

Figure 2. (**a**) Normalized UV-Vis spectra of AuGSH (**black**) and AuGSH-N_3 nanoparticles (**red**) without surface plasmon resonance band (would occur around 530 nm). (**b**) UV-Vis spectra of AuFAM (**green**) and AuAF647 nanoparticles (**blue**).

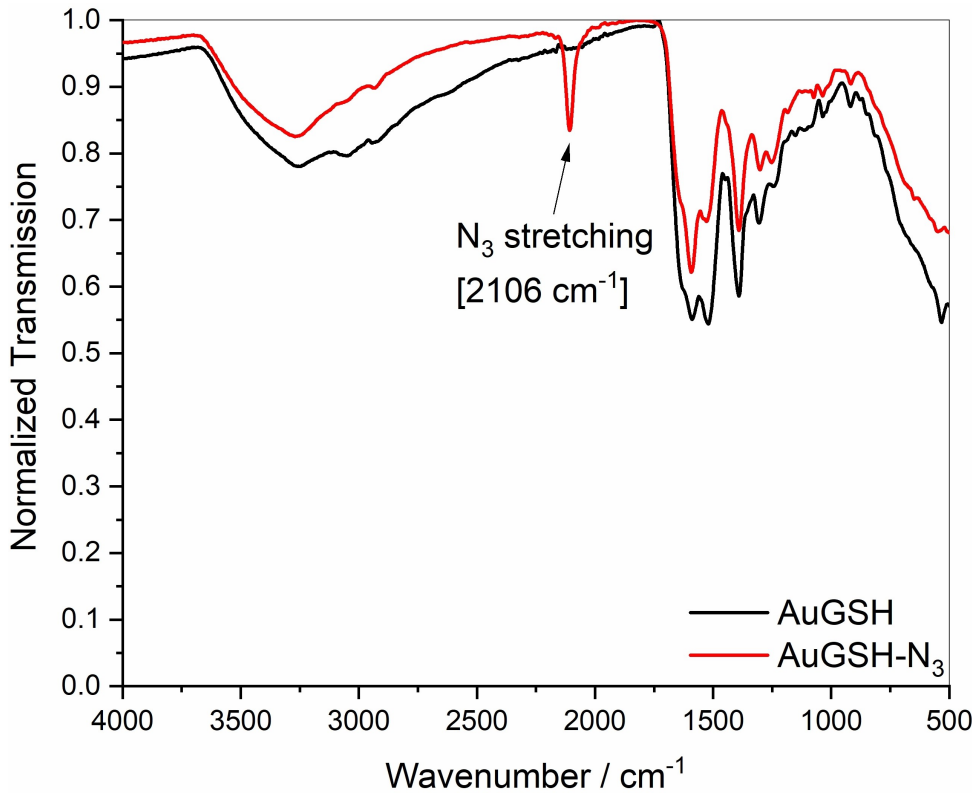

Figure 3. IR spectra of AuGSH and AuGSH-N_3 nanoparticles. The prominent azide band at 2106 cm^{-1} in AuGSH-N_3 nanoparticles indicates the successful surface modification. The carbonyl/amide bands between 1400 and 1600 cm^{-1} did not change significantly as expected.

depicted in Figure 1 (see Supporting Information; Figures S1 to S9). The number of ligands on each gold nanoparticle was determined by a combination of atomic absorption spectroscopy (AAS) and ^{1}H-NMR spectroscopy. AAS gave the molar gold concentration in a given dispersion of surface-functionalized gold nanoparticles which was then be converted into the molar concentration of gold nanoparticles, assuming an average diameter of 2 nm as determined by HRTEM. Quantitative ^{1}H-NMR spectroscopy with the internal calibration standard maleic acid then gave the concentration of GSH molecules (Figure S5). The combination of both values gave the number of GSH molecules per nanoparticle, in that case 125. A spherical

© 2021 The Authors. ChemNanoMat published by Wiley-VCH GmbH

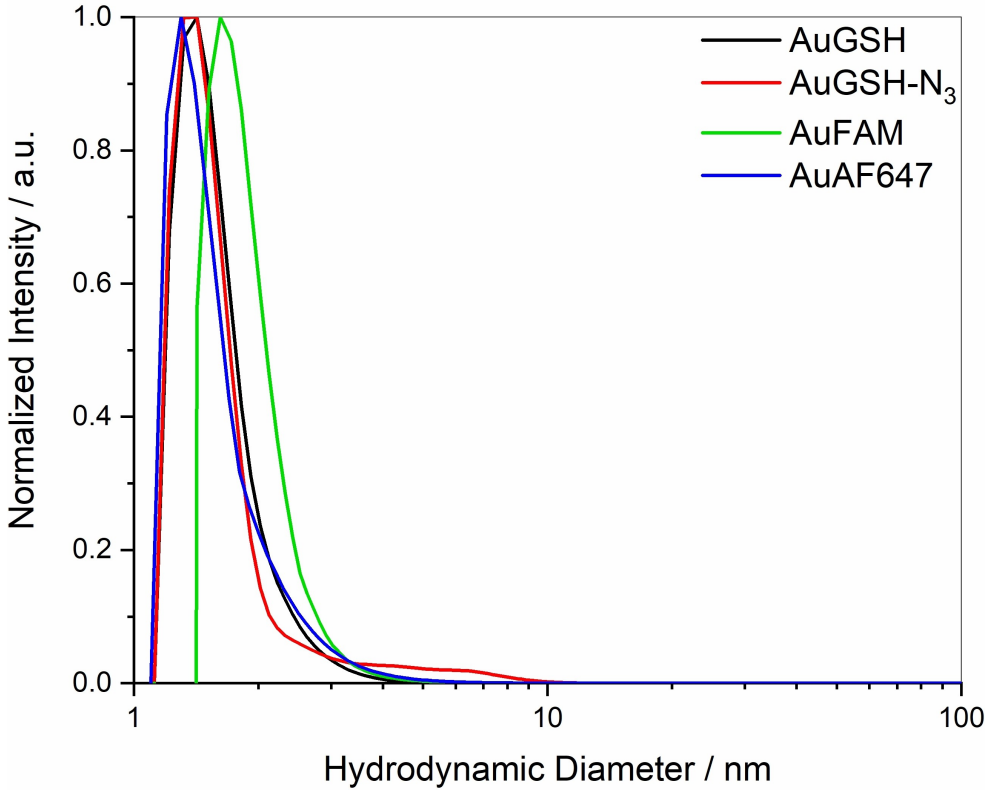

Figure 4. Disc centrifugal sedimentation (DCS) of AuGSH (**black**), AuGSH-N_3 (**red**), AuFAM (**green**), and AuAF647 nanoparticles (**blue**). The hydrodynamic diameter of all particles was in the ultrasmall size range.

2 nm gold nanoparticle contains about 250 gold atoms,[18] therefore the stoichiometry of a particle is approximately $Au_{\sim 250}GSH_{\sim 125}$. With respect to the elemental composition, we can estimate a molecular weight of $250 \cdot 197 + 125 \cdot 306.3 = 87{,}538\ g\,mol^{-1}$. Thus, the gold content in each nanoparticle is about 56 wt%.

The quantification of the azidation was only possible with a 2D ^{1}H-^{13}C-HSQC NMR spectrum (Figure S3) to separate the NMR peaks. The azidation had occurred with a yield of 94%, i.e. each gold nanoparticle carried 118 azidated GSH molecules. Only few amine groups were left. Given the fact that most molecules that shall be clicked to a gold nanoparticle will be larger than a GSH molecule, there are more than enough azide groups as anchoring sites for any subsequent click reaction. The molecular footprint of GSH was 0.20 nm^2 and of GSH-N_3 0.11 nm^2, respectively (Table 1). This agrees well with earlier data on GSH on ultrasmall silver nanoparticles (0.08 nm^2[17a]) and on cysteine on ultrasmall gold nanoparticles (0.15 nm^2[17b]). Taken together, all data support the successful and almost quantitative surface azidation while keeping the ligand glutathione and the gold nanoparticle core intact. Table 1 and Table 2 summarize all chemical shift data for AuGSH and AuGSH-N_3.

The possibility of a covalent surface functionalization was demonstrated by clicking two alkyne-terminated dyes to the nanoparticle surface, respectively. Figure 7 shows the two dye-functionalized nanoparticle systems.

NMR spectroscopy confirmed the attachment of the dye molecules, including the vanishing of the alkyne proton and the evolution of a triazole proton (Figure S10). The absence of sharp peaks in the NMR spectra confirmed the absence of unbound dye molecules. As the NMR spectra of the dye-clicked nanoparticles were rather crowded and the number of dye molecules was small due to steric hindrance, a quantitative determination of the number of dye molecules on the nano-

Table 1. Chemical shift data (peak maxima) of all protons from ^{1}H NMR spectroscopy according to Figure 6.

Compound	H1	H3	H4	H4'	H5	H5'	H6
AuGSH	3.82	3.40	2.59	/	2.19	/	3.83
AuGSH-N_3	3.80	3.39	2.52	2.74	1.99	2.16	3.99

Table 2. Chemical shift data (peak maxima) of all carbon atoms from ^{13}C NMR spectroscopy (taken from Figures S3 and S6).

Compound	C1	C2	C3	C4	C5	C6	C7	C8	C9	C10
AuGSH	43.9	56.4	34.9	31.6	26.5	54.5	171.3	174.4	174.7	176.5
AuGSH-N_3	43.7	56.3	35.2	32.5	27.8	64.9	171.0	175.3	176.3	177.2

© 2021 The Authors. ChemNanoMat published by Wiley-VCH GmbH

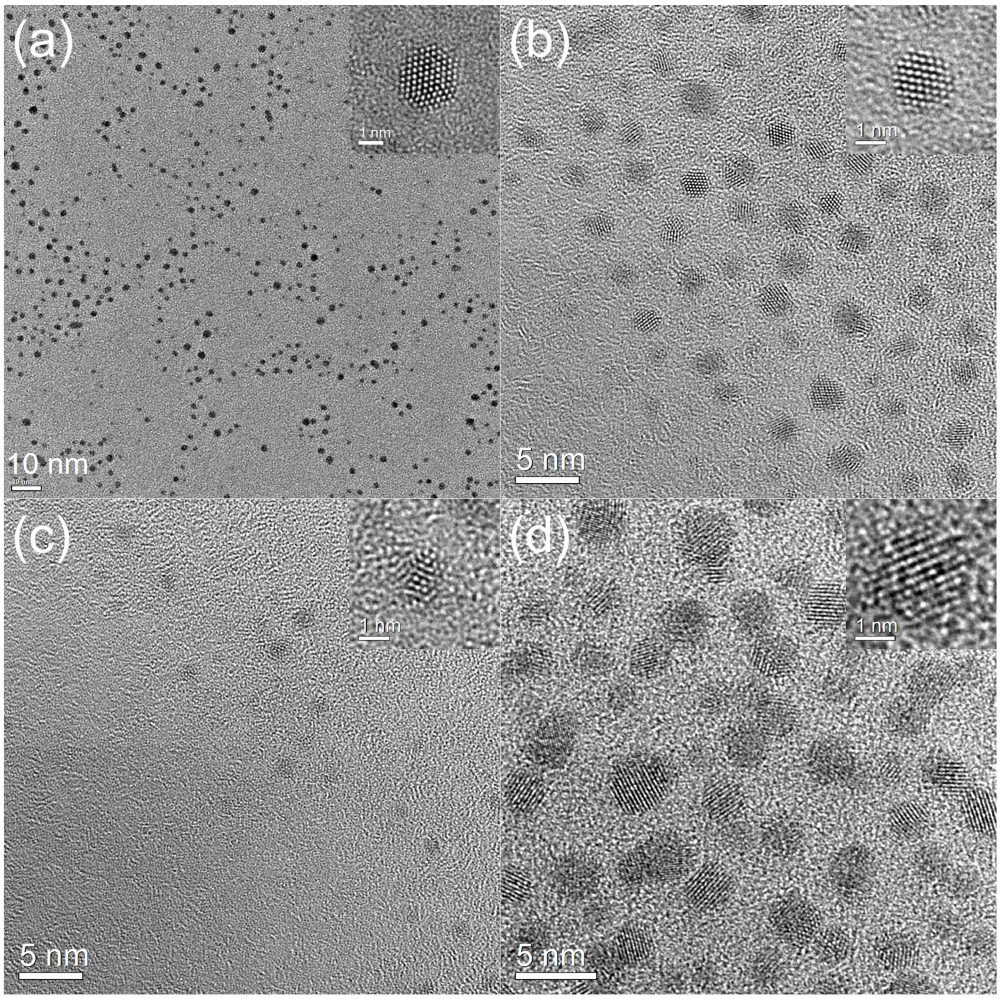

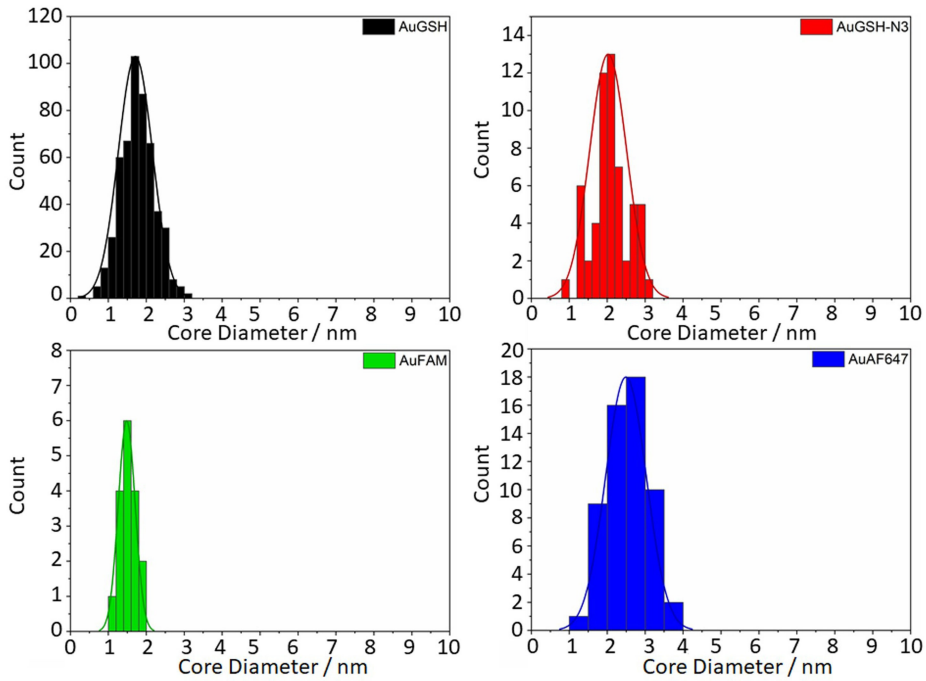

Figure 5. Top: High-resolution transmission electron micrographs of AuGSH **(a)**, AuGSH-N_3 **(b)**, AuFAM **(c)**, and AuAF647 nanoparticles **(d)**. Each inset shows a magnification of one nanoparticle with atomic resolution. **Bottom**: Particle size distribution data.

© 2021 The Authors. ChemNanoMat published by Wiley-VCH GmbH

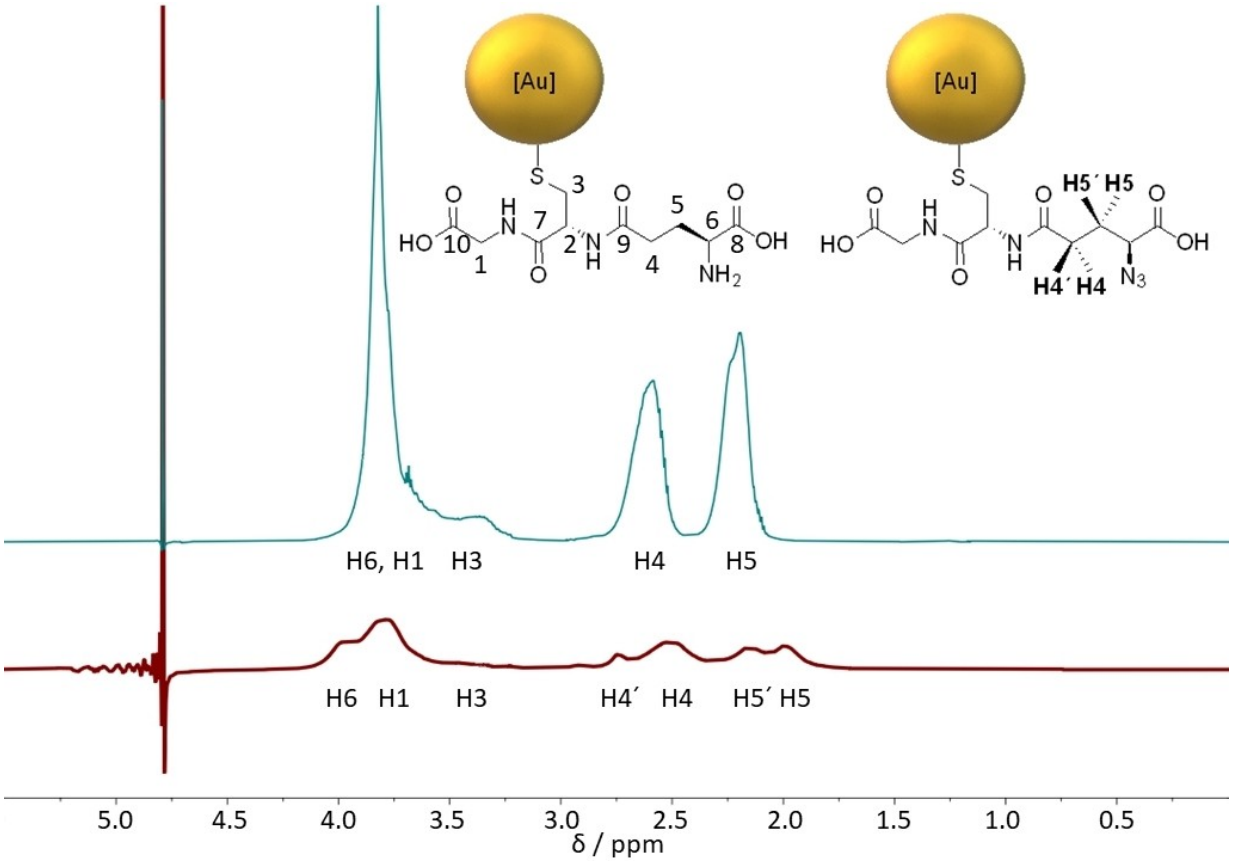

Figure 6. ^{1}H-NMR spectra of AuGSH (**blue**) and AuGSH-N_3 nanoparticles (**red**). Note the broad NMR peaks especially for hydrogen atoms close to the gold core. The proton H2 is below the water suppression.[17a]

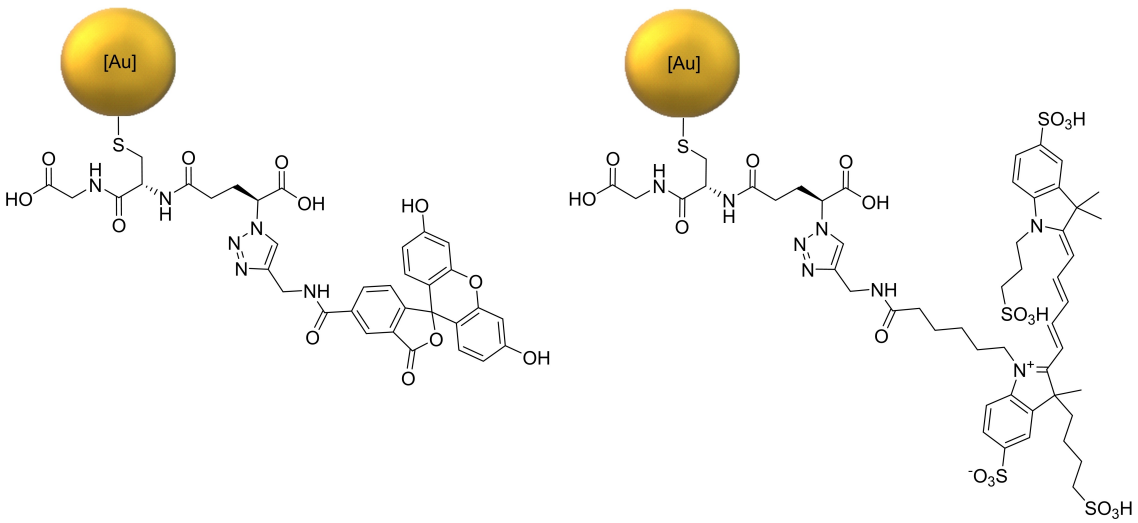

Figure 7. Dye-conjugated gold nanoparticles after CuAAC of AuGCH-N_3 azide-terminated nanoparticles with FAM-alkyne (**left**) and AF647-alkyne (**right**), denoted as AuFAM and AuAF647 in the following.

particle surface was not possible by NMR spectroscopy. Therefore, we analyzed the dispersed nanoparticles by UV-VIS spectroscopy (Figure 2) and by AAS spectroscopy. The first method gave the concentration of dye molecules, the second the concentration of gold nanoparticles. Again, we assumed an average diameter of 2 nm and a spherical shape for the gold nanoparticles. This is reasonable because DCS curves (Figure 4) showed that the particle size had not increased, in accordance

© 2021 The Authors. ChemNanoMat published by Wiley-VCH GmbH

with our earlier studies in the surface functionalization of ultrasmall gold nanoparticles. We found 6 FAM molecules and 11 AF647 molecules per nanoparticle, respectively. The particles were strongly fluorescent after attaching the dyes (Figure 8), i.e. the degree of quenching, if any, was very low.

For clicking, we used 0.4 equivalents of the alkyne-terminated dye with respect to the concentration of azide groups. As each nanoparticle carried 118 azide groups, the clicking efficiency was $6/(118\cdot0.4)=13\%$ for FAM and $11/(118\cdot0.4)=23\%$ for AF647, i.e. only a relatively small fraction of the offered dye-alkyne was actually attached to the surface. We assume that this is due to a steric hindrance on the nanoparticle surface and possibly also to electrostatic repulsion between the dye molecules. The molecular footprint, based on a nanoparticle diameter of 2 nm and a surface area per nanoparticle of $4\pi r^2=12.6\ nm^2$, was 2.1 nm^2 for FAM and 1.15 nm^2 for AF647. In earlier studies, FAM had a footprint of 1.48 nm^2[8b,19] and Cy3 had a footprint of 2.5 nm^2,[19] both after clicking to ultrasmall gold nanoparticles decorated with the K(N_3)CD tripeptide. This supports the assumption that the number of dye molecules is not limited by the available azide groups but by steric crowding or electrostatic repulsion between the dye molecules.

Table 3 summarizes all analytical data of the surface-conjugated nanoparticles. The individual reaction steps occur with high yield and do not affect the size of the gold core. This demonstrates that the synthetic route presented here leads to the same results as reported earlier, but on a scale of more than 100 times larger than the synthesis reported earlier, where the K(N_3)CD peptide was used as coupling agent.[8] The synthetic route presented here is applicable to the covalent surface functionalization of noble metal nanoparticles, e.g. to use them for imaging[19] or biological targeting.[8a]

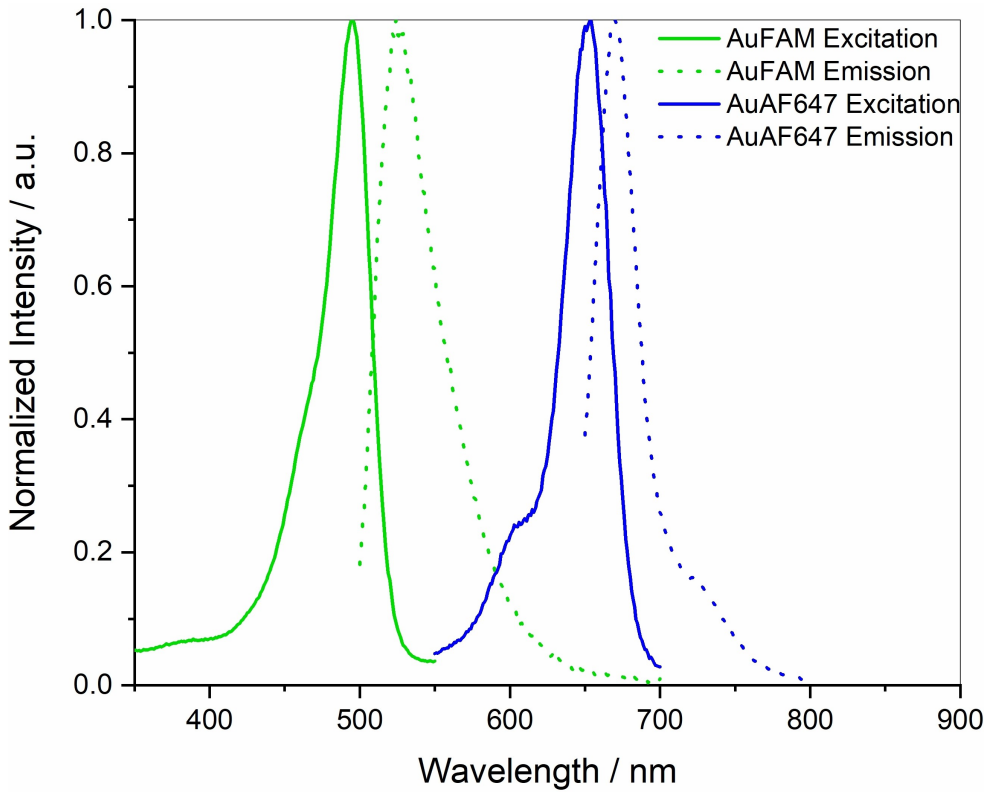

Figure 8. Normalized fluorescence spectra of dye-functionalized gold nanoparticles. AuFAM nanoparticles emit at 532 nm, and AuAF647 nanoparticles emit at 676 nm.

Table 3. Analytical data of AuGSH, AuGSH-N_3, AuFAM, and AuAF647 nanoparticles. The calculations were all based on an average particle diameter of 2 nm to allow a better comparison. The yield of each step was individually calculated by the parent compound concentration (particles) for each functionalization.

Particle	Hydrodynamic diameter by DCS/nm	Metallic core diameter by HRTEM/nm	Nanoparticle yield (based on Au)/%	Number of ligands per nanoparticle	Molecular footprint per ligand/nm^2	Reaction efficiency/%
AuGSH	1.5 ± 0.2	1.7 ± 0.9	72	125	0.10	–
AuGSH-N_3	1.5 ± 0.2	2.0 ± 0.4	86	118	0.11	94 (azidation)
AuFAM	1.8 ± 0.3	1.5 ± 0.5	89	6	2.1	13 (CuAAC)
AuAF647	1.4 ± 0.2	2.5 ± 1.1	87	11	1.15	23 (CuAAC)

© 2021 The Authors. ChemNanoMat published by Wiley-VCH GmbH

Conclusions

A stable surface functionalization of ultrasmall gold nanoparticles is possible after azidation of surface-bound GSH, followed by copper-catalyzed azide-alkyne click reaction. Both steps occur with high yield, giving a pathway for a versatile and convenient attachment of all kinds of molecules that carry an alkyne group. This synthetic method should be easily transferable to other metal nanoparticles that have strong metal-sulfur bonds, like silver or platinum metals. Of course, it can also be used to functionalize larger metallic nanoparticles with the drawback that an analysis of the attached molecules by NMR (too broad peaks) or fluorescence spectroscopy (quenching) is no longer possible. However, it is reasonable to assume that the reactions occur with the same efficiency for larger nanoparticles as well. The detailed analysis of the nanoparticle surface that has been carried out for ultrasmall nanoparticles should be transferable to larger nanoparticles.

Experimental Section

Chemicals

Hydrochloric acid (HCl, 37%), nitric acid (HNO_3, 67%), and sodium hydroxide (NaOH, 1 M) were purchased at Bernd Kraft (Duisburg, Germany). Sodium borohydride ($NaBH_4$, 99%) and 3 kDa spin filters were purchased at Merck (Darmstadt, Germany). Glutathione (GSH, 98%), maleic acid (99%), potassium carbonate (K_2CO_3, 99%), copper sulfate ($CuSO_4$, 98%), tris(3-hydroxypropyl-triazolylmethyl) amine (THPTA, 96%) and sodium ascorbate (99%) were purchased at Sigma-Aldrich (Steinheim, Germany). Deuterium oxide (D_2O, 99.9%) was purchased at Deutero GmbH (Kastellaun, Germany). Methanol (99.8%) was purchased at Fisher Scientific (Geel, Belgium). Aminoguanidine hydrogen carbonate (98%) was purchased at Alfa Aesar (Kandel, Germany). Dimethyl sulfoxide (DMSO, 97%) was purchased at AppliChem (Darmstadt, Germany). FAM-alkyne (95%) was purchased at Lumiprobe (Hannover, Germany), and AF647-alkyne (95%) was purchased at Jena Bioscience (Jena, Germany). Sucrose (99%) was purchased at VWR Chemicals (Langenfeld, Germany). Dodecane (99%) and the PVC nanoparticle calibration dispersion (Lot#149, 1.385 g L^{-1}) were purchased at CPS Instruments Inc. (Oosterhout, The Netherlands).

All syntheses were carried out with ultrapure water (Purelab ultra instrument, ELGA) and at ambient temperature unless otherwise noted. All glassware was boiled previously with *aqua regia* and thoroughly rinsed with ultrapure water.

Instruments

UV-Vis spectra were recorded on a Genesis 50 instrument (ThermoScientific) in quartz glass cuvettes in the range of 200 nm to 800 nm. Atomic absorption spectroscopy (AAS) was done with an Electron M-Series spectrometer (ThermoScientific). 10 µL of the nanoparticle dispersion was dissolved in 990 µL *aqua regia* and then diluted with 4 mL water before the analysis. NMR spectra were measured on an Avance III instrument (Bruker). The 2D spectra are combinations of ^{1}H and ^{13}C spectra measured on an AV Neo 600 MHz instrument (Bruker). The spectra of imidazole-1-sulfonyl azide hydrogen sulfate were measured on an AV Neo 400 MHz instrument (Bruker). For NMR spectroscopy, the nanoparticles were dispersed in a mixture of 90% H_2O/10% D_2O with suppression of the water signal at pH 8. A typical nanoparticle concentration for 1D and 2D NMR spectra was 260 µM (12.6 g L^{-1} Au) in a volume of 600 µL. Disc centrifugal sedimentation (DCS) was carried out with a DC24000 instrument (CPS). The disc was accelerated to 24000 rpm, then a gradient of sucrose solution was injected. Starting with 1.6 mL of 24 wt% sucrose in water, the gradient increased in steps of 0.2 mL to 1.6 mL of 8 wt% sucrose in water. The gradient solution was capped with 0.5 mL of dodecane to avoid evaporation. The instrument was calibrated with a dispersion of stabilized PVC particles with a defined hydrodynamic diameter of 483 nm. Infrared (IR) spectra were recorded on an Alpha-Platinum ATR spectrometer (Bruker) with freeze-dried samples. The samples were freeze-dried with an Alpha 2–4 LSC instrument (Christ).

High-resolution transmission electron microscopy (HRTEM) was done with an aberration-corrected FEI Titan transmission electron microscope equipped with a Cs-probe corrector (CEOS Company), operating at 300 kV.[20] 20 µL of nanoparticle dispersion was drop-cast on a copper grid, coated with an ultra-thin amorphous carbon film.

Synthesis of nanoparticles

Glutathione-functionalized nanoparticles (AuGSH) were synthesized by an adapted Brust-Schiffrin synthesis.[5b,21] $HAuCl_4$ was prepared by dissolution of elemental gold in *aqua regia*. In a typical synthesis, 4 mL of an $HAuCl_4$ solution (203 µmol, 40 mg Au) were diluted to 200 mL with water. Glutathione (4 eq., 812 µmol, 250 mg) was dissolved in 10 mL ice-cold water and added to the gold solution, which instantly changed its color to milky white. After 10 min stirring, 4 mL of a freshly prepared ice-cold $NaBH_4$ solution (4 eq., 200 mM; 7.6 g L^{-1}) was added to the reaction. The color of the reaction mixture changed to dark brown. The reaction mixture was stirred for 10 min and then left unstirred for 30 min. After that time, a dark brown precipitate had sedimented from the solution which was then isolated at 4,000 rpm (2500 g; 30 min). The precipitate was redispersed in 10 mL 0.1 M NaOH, and the volume was decreased to 1 mL by spin filtration in 3 kDa Amicon spin filters at 4000 rpm for 60 min. Up to 50 mg of GSH-functionalized ultrasmall gold nanoparticles were obtained (yield 70–80% with respect to the gold content by AAS).

Azidation of AuGSH nanoparticles was performed as follows. In the first syntheses, we measured the concentration of gold by AAS to ensure a constant reproducibility, but later-on, we tentatively assumed a yield of 80% with respect to gold as the prior synthesis was well reproducible. AuGSH nanoparticles with 5 mg gold (0.10 µmol NPs, 12.85 µmol GSH) were dispersed in 6 mL water. 18 mL methanol were added to the dispersion. Subsequently, imidazole-1-sulfonyl azide hydrogen sulfate (50 eq. to GSH, 642 µmol, 175 mg) was dissolved in 1 mL water and added to the mixture, which instantly turned brown and cloudy. K_2CO_3 (50 eq. to GSH, 642 µmol, 87.5 mg) was dissolved in 1 mL water and added to the reaction mixture. To start the reaction, 1 mL of an aqueous solution of $CuSO_4$ (0.39 eq to GSH, 5 µmol mL^{-1}) was added. The cloudy dispersion became transparent after the subsequent addition of 1 mL aqueous NaOH (1 M) and 9 mL water to give a final ratio of 1:1 methanol to water. The reaction mixture was stirred for 48 h at room temperature and then washed by spin filtration with ultrapure water 6 times for 45 min at 4,000 rpm (2500 g). The AuGSH-N_3 nanoparticles were then used for further functionalization and analysis.

Clicking of alkyne-terminated molecules to AuGSH-N_3 was carried out as follows. A sample containing 7.7 µmol azido groups on AuGSH-N_3 nanoparticles (1 eq, 68 nmol AuGSH-N_3, 3.15 mg Au) was dispersed to 3 mL with water. The alkyne-terminated dye was then

© 2021 The Authors. ChemNanoMat published by Wiley-VCH GmbH

rapidly added. Fluorescein alkyne (FAM-alkyne, 0.4 eq, 3.16 μmol, 1.30 mg) was dissolved in 1 mL NaOH (0.1 M) solution. Alexa fluorophore 647 alkyne (AF647-alkyne, 0.4 eq, 3.16 μmol, 2.86 mg) was dissolved in 1 mL DMSO. After addition of the alkyne-dye, respectively, 630 μL of an aqueous solution of a complex of Cu^{2+} and tris((1-hydroxy-propyl-1H-1,2,3-triazol-4-yl)methyl)amine (THPTA) (0.08 eq. Cu, 0.4 eq. THPTA) was added. This solution was prepared beforehand by dissolving $CuSO_4$ (10 μmol, 1.6 mg) in 10 mL water together with THPTA (50 μmol, 21.7 mg) and aminoguanidine hydrogen carbonate (10 μmol, 1.4 mg). After adding the copper/THPTA solution, sodium ascorbate (3.15 μmol, 0.63 mg in 100 μL water) was added to induce the reaction. Subsequently, the reaction mixture was vigorously stirred for 14 h, diluted with water (20 mL), and purified by 4 times spin filtration at the same conditions as for AuGSH.

Synthesis of Imidazole-1-sulfonyl azide hydrogen sulfate

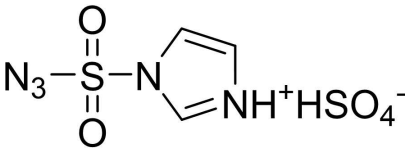

Safety advice: Note the precautionary statements given below. All synthetic procedures were carried out under Argon (Schlenk technique). Imidazole-1-sulfonyl azide hydrogen sulfate was synthesized according to ref.[14b] with slight modifications. A 500 mL round-bottom flask was first flushed three times with argon to exclude water. Then, sodium azide (15 g, 231 mmol) was added and suspended in dry ethylacetate (231 mL, 1 mmol mL^{-1}). The flask was sealed under argon and cooled to 0 °C with an ice bath. Sulfurylchloride (1 eq., 18.7 mL, 231 mmol) was very slowly added dropwise during 15 min. During this addition, the milky white suspension slowly turned yellow. Afterwards, the suspension was allowed to warm to room temperature for 20 h. Then, the yellow color had been replaced with a yellow-orange color. The suspension was re-cooled to 0 °C with an ice bath before imidazole (1.9 eq., 30 g, 440 mmol, solid powder) was slowly added during 15 min under inert gas conditions. The orange suspension turned into a deep-orange slurry dispersion during stirring for 3.5 h at 0 °C (ice bath). Then, a saturated solution of sodium bicarbonate solution (200 mL) was added slowly to minimize the resulting bubbling. After the formation of gas had ceased, the pH was checked to ensure a basic pH (>9). The orange solution was then transferred into a separatory funnel and the organic layer was isolated. The orange layer of ethylacetate was washed once with water and once with saturated aqueous sodium chloride, respectively. The colorless layer of ethylacetate was dried with magnesium sulfate, filtrated and transferred into a 500 mL round-bottom flask. The flask was flushed with argon, sealed under inert gas atmosphere, and cooled to 0 °C with an ice bath. To precipitate the product, concentrated sulfuric acid (1 eq, 12.3 mL, 231 mmol) was added dropwise during 15 min. The product precipitated as white solid. The suspension was stirred for another hour on ice and then gradually warmed to room temperature during 1 h. The product was collected by vacuum filtration and dried in oil-pump vacuum. The yield was 46 g (73%) of a white solid.

Characterization: ^{1}H-NMR (400 MHz, D_2O): δ/ppm = 9.24 (s, 1H), 7.74 (d, 1H), 7.38 (d, 1H) (Figure S11). ^{13}C-NMR (400 MHz, D_2O): δ/ppm = 137.70, 123.79, 119.96 (Figure S12). IR (ATR, solid): $\tilde{\upsilon}_{max}$/cm^{-1} = 2176 (N_3), 1301 (S=O), 1125 (S=O) (Figure S13). HR-MS (ESI-pos.) *m/z*: Calculated for $[C_3H_3N_5O_2S+H]^+$: 174.0080, found 174.0078 g mol^{-1}.HR-MS (ESI-neg.) *m/z*: Calculated for $[HSO_4]^-$: 96.9601, found 96.9603 g mol^{-1}.

Precautionary statements: To avoid the formation of hydrazoic acid, HN_3, the pH must always be kept alkaline when handling sodium azide during the rection. As an azido compound imidazole-1-sulfonyl azide is a potentially explosive liquid. Stick et al. introduced its hydrochloride salt[14a,22] which can be handled much more safely. However, the hydrochloride salt is very hygroscopic and not suitable for prolonged storage even under argon.[23] When salt gets wet and aged, black crystals can form under the formation of HN_3 gas which is highly explosive and toxic. So, in general, if black crystals in the product are observed during any time of the synthesis, the batch must be immediately discarded. For a safe disposal, the crystals should be dissolved in water and aqueous solutions of 0.1% $Na_2S_2O_3$ (7.88 mM) and 0.2% KI/I_2 (7.88 mM each) should be added (reduction of azide to amine). A slight bubbling of N_2 can be observed during the addition of both solutions. After the bubbling has ceased, the mixture can be discarded as alkaline aqueous waste.

As alternative to the unstable hydrochloride salt, Gardiner et al. proposed a new synthesis of the hydrogensulfate salt.[14b] This was tested for its stability by mechanical shock, grinding, and heating up to its melting point of 375..378 K and considered as stable compound. In our hands, the hydrogensulfate salt was stable without any color change during storage during more than 18 months at 5 °C (fridge) under inert gas atmosphere (argon).

Acknowledgements

The authors acknowledge financial support of this work by the Deutsche Forschungsgemeinschaft SFB/CRC 1093: Supramolecular chemistry on proteins. We thank Dr Felix Niemeyer and Dr Torsten Schaller for NMR spectroscopic measurements. We thank Robin Meya and Beate Römer for elemental analysis. Open Access funding enabled and organized by Projekt DEAL.

Conflict of Interest

The authors declare no conflict of interest.

Keywords: Gold · nanoparticles · click chemistry · surface functionalization

[1] K. Zarschler, L. Rocks, N. Licciardello, L. Boselli, E. Polo, K. P. Garcia, L. De Cola, H. Stephan, K. A. Dawson, *Nanomedicine* **2016**, *12*, 1663–1701.
[2] K. Wey, M. Epple, *J. Mater. Sci. Mater. Med.* **2020**, *31*, 117.
[3] a) H. Häkkinen, *Nat. Chem.* **2012**, *4*, 443–455; b) F. Bensebaa, Z. Yu, Y. Deslandes, E. Kruus, T. H. Ellis, *Surf. Sci.* **1998**, *405*, L472–L476; c) J. R. Reimers, M. J. Ford, S. M. Marcuccio, J. Ulstrup, N. S. Hush, *Nat. Chem. Rev.* **2017**, *1*, 0017.
[4] a) V. Andermark, K. Göke, M. Kokoschka, M. A. el Abu Maaty, C. T. Lum, T. Zou, R. W. Y. Sun, E. Aguilo, L. Oehninger, L. Rodriguez, H. Bunjes, S. Wölfl, C. M. Che, I. Ott, *J. Inorg. Biochem.* **2016**, *160*, 140–148; b) G. S. P. Garusinghe, S. M. Bessey, M. Aghamoosa, M. McKinnon, A. E. Bruce, M. R. M. Bruce, *Inorganics* **2015**, *3*, 40–54; c) K. Konishi, in *Gold Clusters, Colloids and Nanoparticles I, Vol. 161* (Ed.: D. M. P. Mingos), Springer, **2014**, pp. 49–86; d) Z. Assefa, J. M. Forward, T. A. Grant, R. J. Staples, B. E. Hanson, A. A. Mohamed, J. P. Fackler, *Inorg. Chim. Acta* **2003**, *352*, 31–45.
[5] a) M. Azubel, R. D. Kornberg, *Nano Lett.* **2016**, *16*, 3348–3351; b) L. M. Liz-Marzán, *Chem. Commun.* **2013**, *49*, 16–18; c) I. Hussain, S. Graham, Z. Wang, B. Tan, C. C. Sherrington, S. P. Rannard, A. I. Cooper, M. Brust, *J.*

© 2021 The Authors. ChemNanoMat published by Wiley-VCH GmbH

Am. Chem. Soc. **2005**, *127*, 16398–16399; d) M. Brust, C. J. Kiely, *Coll. Surf. A* **2002**, *202*, 175–186; e) M. Brust, M. Walker, D. Bethell, D. J. Schiffrin, R. Whyman, *Chem. Commun.* **1994**, 801–802.
[6] W. R. Algar, D. E. Prasuhn, M. H. Stewart, T. L. Jennings, J. B. Blanco-Canosa, P. E. Dawson, I. L. Medintz, *Bioconjugate Chem.* **2011**, *22*, 825–858.
[7] a) S. B. van der Meer, T. Seiler, C. Buchmann, G. Partalidou, S. Boden, K. Loza, M. Heggen, J. Linders, O. Prymak, C. L. P. Oliveira, L. Hartmann, M. Epple, *Chem. Eur. J.* **2021**, *27*, 1451–1464; b) T. Ruks, K. Loza, M. Heggen, O. Prymak, A. L. Sehnem, C. L. P. Oliveira, P. Bayer, C. Beuck, M. Epple, *ACS Appl. Bio Mater.* **2021**, *4*, 945–965; c) T. Ruks, K. Loza, M. Heggen, C. Ottmann, P. Bayer, C. Beuck, M. Epple, *ChemBioChem* **2021**, *22*, 1456–1463; d) B. Schuetze, C. Mayer, K. Loza, M. Gocyla, M. Heggen, M. Epple, *J. Mater. Chem. B* **2016**, *4*, 2179–2189.
[8] a) S. B. van der Meer, I. Hadrovic, A. Meiners, K. Loza, M. Heggen, S. K. Knauer, P. Bayer, T. Schrader, C. Beuck, M. Epple, *J. Phys. Chem. B* **2021**, *125*, 115–127; b) S. B. van der Meer, K. Loza, K. Wey, M. Heggen, C. Beuck, P. Bayer, M. Epple, *Langmuir* **2019**, *35*, 7191–7204.
[9] a) Y. Li, R. Juarez-Mosqueda, Y. Song, Y. Zhang, J. Chai, G. Mpourmpakis, R. Jin, *Nanoscale* **2020**, *12*, 9423–9429; b) X. F. Zan, Q. Z. Li, Y. T. Pan, D. J. Morris, P. Zhang, P. Li, H. Z. Yu, M. Z. Zhu, *ACS Appl. Nano Mater.* **2018**, *1*, 6773–6781; c) R. Dinkel, W. Peukert, B. Braunschweig, *J. Phys. Condens. Matter* **2017**, *29*, 133002; d) E. Reyes, R. Madueño, M. Blázquez, T. Pineda, *J. Phys. Chem. C* **2010**, *114*, 15955–15962.
[10] a) M. Fischler, A. Sologubenko, J. Mayer, G. Clever, G. Burley, J. Gierlich, T. Carell, U. Simon, *Chem. Commun.* **2008**, 169–171; b) S. Hosseini, O. Wetzel, K. Kostka, M. Heggen, K. Loza, M. Epple, *Molecules* **2021**, *26*, 5069.
[11] J. E. Hein, V. V. Fokin, *Chem. Soc. Rev.* **2010**, *39*, 1302–1315.
[12] H. C. Kolb, M. G. Finn, K. B. Sharpless, *Angew. Chem. Int. Ed.* **2001**, *40*, 2004–2021; *Angew. Chem.* **2001**, *113*, 2056–2075.
[13] a) V. Poonthiyil, T. K. Lindhorst, V. B. Golovko, A. J. Fairbanks, *Beilstein J. Org. Chem.* **2018**, *14*, 11–24; b) Y. P. Chen, Y. L. Xianyu, X. Y. Jiang, *Acc. Chem. Res.* **2017**, *50*, 310–319; c) N. W. Li, W. H. Binder, *J. Mater. Chem.* **2011**, *21*, 16717–16734; d) E. H. Peters, M. Mayor, *Eur. J. Inorg. Chem.* **2020**, *2020*, 2325–2334; e) T. R. Sibakoti, C. R. Stinger, P. K. Adhihetty, F. P. Zamborini, M. H. Nantz, *Part. Part. Syst. Charact.* **2019**, *36*, 1900093; f) W. Mao, H. S. Kim, Y. J. Son, S. R. Kim, H. S. Yoo, *J. Controlled Rel.* **2018**, *269*, 52–62; g) M. Homberger, S. Schmid, J. Timper, U. Simon, *J. Cluster Sci.* **2012**, *23*, 1049–1059; h) N. Gandra, S. Singamaneni, *Chem. Commun.* **2012**, *48*, 11540–11542.
[14] a) E. D. Goddard-Borger, R. V. Stick, *Org. Lett.* **2007**, *9*, 3797–3800; b) G. T. Potter, G. C. Jayson, G. J. Miller, J. M. Gardiner, *J. Org. Chem.* **2016**, *81*, 3443–3446.
[15] a) V. Amendola, R. Pilot, M. Frasconi, O. M. Maragò, M. A. Iatì, *J. Phys. Condens. Matter* **2017**, *29*, 203002; b) J. Langer, S. M. Novikov, L. M. Liz-Marzán, *Nanotechnology* **2015**, *26*, 322001.
[16] H. Fissan, S. Ristig, H. Kaminski, C. Asbach, M. Epple, *Anal. Meth.* **2014**, *6*, 7324–7334.
[17] a) O. Wetzel, S. Hosseini, K. Loza, M. Heggen, O. Prymak, P. Bayer, C. Beuck, T. Schaller, F. Niemeyer, C. Weidenthaler, M. Epple, *J. Phys. Chem. B* **2021**, *125*, 5645–5659; b) T. Ruks, C. Beuck, T. Schaller, F. Niemeyer, M. Zähres, K. Loza, M. Heggen, U. Hagemann, C. Mayer, P. Bayer, M. Epple, *Langmuir* **2019**, *35*, 767–778; c) G. Salassa, T. Burgi, *Nanoscale Horiz.* **2018**, *3*, 457–463; d) C. Guo, J. L. Yarger, *Magn. Reson. Chem.* **2018**, *56*, 1074–1082; e) L. E. Marbella, J. E. Millstone, *Chem. Mater.* **2015**, *27*, 2721–2739.
[18] D. M. P. Mingos, in *Structure and Bonding, Vol. 161*, Springer, Heidelberg, **2014**.
[19] V. Sokolova, G. Nzou, S. B. van der Meer, T. Ruks, M. Heggen, K. Loza, N. Hagemann, F. Murke, B. Giebel, D. M. Hermann, A. J. Atala, M. Epple, *Acta Biomater.* **2020**, *111*, 349–362.
[20] A. Thust, J. Barthel, K. Tillmann, *J. Large-scale Res. Fac.* **2016**, *2*, A41.
[21] M. Brust, J. Fink, D. Bethell, D. J. Schiffrin, C. Kiely, *Chem. Commun.* **1995**, 1655–1656.
[22] E. D. Goddard-Borger, R. V. Stick, *Org. Lett.* **2011**, *13*, 2514–2514.
[23] N. Fischer, E. D. Goddard-Borger, R. Greiner, T. M. Klapötke, B. W. Skelton, J. Stierstorfer, *J. Org. Chem.* **2012**, *77*, 1760–1764.

Manuscript received: September 6, 2021
Revised manuscript received: October 12, 2021
Accepted manuscript online: October 22, 2021
Version of record online: November 8, 2021

© 2021 The Authors. ChemNanoMat published by Wiley-VCH GmbH